

Three-dimensional borehole radar imaging using synthetic aperture time-domain focusing

Pradip K. Mukhopadhyay*, M. R. Inggs, A. J. Wilkinson, R.T.Lord, Radar Remote Sensing Group, Department of Electrical Engineering, University of Cape Town, Rondebosch, 7701, South Africa.

Summary

An imaging algorithm with three-dimensional capability is implemented suitable for processing nonparallel, wideband, VHF borehole radar data. In a real borehole situation it is difficult to build thin, efficient and directional antennas. With axially omnidirectional antennas, there will be ambiguity problems, as the return will come from left and right side of the borehole, which restricts the application of narrow band interferometric height reconstruction techniques. Furthermore, bandwidths of 75% are typical for borehole radar, while narrow band Interferometric Synthetic Aperture Radar (SAR) systems have bandwidths typically less than 5%. In this study, the data is focussed using SAR time-domain processing. The 3D image has been formed by finding the overlap between the intensity images taken from different view angles (i.e. multiple boreholes). The rotational ambiguity with omnidirectional antennas using multiple borehole is discussed. The algorithm has tested on simulated radar data and using sonar data from a acoustic water tank.

boreholes is not economically feasible in deep mines. Using phase interferograms from side-looking, narrow band SAR, a simulation study of 3D imaging has been carried out (Mukhopadhyay et al., 2001). In general bandwidths of 75% are typical for borehole radar while Interferometric SAR (InSAR) systems have bandwidths typically less than 5%, restricting the application of narrow band InSAR height reconstruction techniques in a borehole environment.

Thin borehole radars are cylindrically omnidirectional. Thus, reflection comes from left and right side of the borehole in equal slant range, which will cause ambiguities due to the superposition of the signals. In the real borehole situation, the trajectories are neither parallel to each other nor straight. A time-domain SAR algorithm is well suited to the focusing of data acquired along a curved trajectory.

In this paper, we will first present the image formation technique, the resolution and sampling criteria, and the results achieved via numerical simulation, as well as from experimental data obtained from a small-scale acoustic tank.

Introduction

For efficient mine planning and economic assessment, knowledge of subsurface structures ahead of mining in 3D and with high resolution is very useful. Tools such as 3D seismology have been adapted from the oil industry and applied to the planning of ultra-deep mines, but these tools lack the resolution to reveal <20 m features that hazard mine workings (Pretorius et al., 1997). Three-dimensional orebody geometry estimates derived from coring never have sufficient detail, due to lateral inhomogeneity. Trials in mines have established that wideband VHF borehole radars, working in the 10-100 MHz band, can be used to probe the rockmass between boreholes over ranges from <5m to as much as 150m with submetre resolution (Mason et al., 2001).

An imaging system with three-dimensional capability has been implemented by using a stepped frequency radar which synthesizes a two-dimensional aperture (Lopez-Sanchez et al, 2000). 2D aperture synthesis requiring many

Formulation of the 3-D Image

Focusing Algorithm

The basic SAR image focusing technique can be discussed using the idealised case of an object embedded in a homogeneous medium. As illustrated in Figure 1, moving an antenna operating in a monostatic mode past the object position P allows collection of data for the formation of the synthetic aperture. Let the received waveform for the nth position of the antenna be $s_n(t)$,

where $t = 2r_n/v$ is the two way travel time, $r_n = \sqrt{(x-x_n)^2 + (y-y_n)^2 + (z-z_n)^2}$ is the distance from the nth antenna position to the scatterer point (x,y,z) and v is the propagation velocity in the medium.

The formation of the focused image consists of range focusing and azimuth focusing. The range focusing is achieved by convolving each received echo with a matched filter, which is simply the time-reversed, complex conjugate of the transmitted waveform. Azimuth focusing is more difficult, mainly because of the range migration

Three-dimensional borehole radar imaging using synthetic aperture time-domain focusing

problem, which means that a point scatterer's signal does not remain in one range bin over the integration length. A time-domain SAR processor calculates the expected signal trajectory in the data matrix for each scatterer, and then applies the appropriate phase correction along the signal trajectory before doing the integration in time-domain (Bamler et al., 1998)

3-D Image formation using multiple SAR focused image

A 3D image of the scene can be constructed by combining the received signal intensity from different boreholes as

$$G(x,y,z) = |A(x_a,t_a)| * |B(x_b,t_b)|$$

where the analytical signal $A(x_a,t_a)$ is from borehole A, and $B(x_b,t_b)$ is from borehole B.

Each point scatterer will be projected in different azimuth and slant range positions in different images. A grid of (x,y,z) points is defined for the imaged scene. For each point in the grid, the azimuth and slant range positions are calculated in each image and the corresponding intensity values are multiplied to get resultant $G(x,y,z)$. We will get a high value of $G(x,y,z)$ in a grid position (x,y,z) if there is a point scatterer present at (x,y,z) . Multiplication of two signals will give non-zero value where the two signals overlap (Mason et al. 2001). In a real situation we will never get zero value of G , the presence of a target is indicated when some threshold is exceeded.

Resolution and sampling criteria

The resolution obtained in the reconstructed image is dependent upon bandwidth, antenna beamwidth, and the medium parameters.

The range resolution (Δr) depends upon the pulse bandwidth and the propagation velocity since $\Delta r \approx v/2B$, where B is the bandwidth.

The cross-range resolution is $\Delta x \approx 1/B_x$, where $B_x = 4 * \sin(\theta/2) / \lambda$, where θ is the azimuth beamwidth and λ the wavelength at center frequency.

So the sampling interval along the slant range must be less than Δr . The sampling interval along the azimuth must be less than Δx .

Results and discussions

The numerical simulations shown here correspond to the dimensions of experimental results obtained using an acoustic model of the real mine situation¹.

Numerical Simulations

Figure 2. shows a sketch of the target used in the numerical simulation. The radar is "flying" at a height of 150 mm/sec in three flight paths, one along the X axis and the other two making 10° & 15° angle with the X axis. Synthetic apertures were built up by collecting traces at 0.76 mm intervals along each line. The 10 isotropic point scatterers are placed in different X,Y,Z locations. The X positions are at 38 mm and 76 mm, Y positions are from 70 mm to 90 mm with an interval of 5 mm and Z positions are from 40 mm to 0 mm with an interval of 5 mm. The azimuth and range beamwidths are both 30° . ²The bandwidth is 1.25 MHz and we have a constant propagation velocity of 1486 m/sec. Figure 3(a), (b) & 3(c) shows the simulated range-focused images with 10 symmetrical diffraction hyperbolas present. Figure 4(a), (b) & (c) shows the focussed image which shows 10 scatterers in slant range. Figure 5. shows the reconstructed 3D image of the desired scene.

Experimental Results

Figure 6 shows a model of five 6 mm diameter aluminum spheres placed on the end of long pins. The mount for the spheres was composed of several sheets of Perspex and contained a regular grid of holes to allow for the position of the pins to be changed. The model is placed in a water-filled tank. The time section shown in Figure 7(a) and (b) were collected by scanning a 25 mm diameter, 50 mm focal length broadband 0.75–1.5 MHz ultrasonic transducer over the half sphere in two lines, making 30° angle to each other. Synthetic apertures were built up by collecting traces at 0.76 mm intervals along each line. At each station, the transducer was rocked about its focal point (to simulate the broad axial beamwidth of the real radar) and the echoes were stacked.

Figure 8(a) and (b) shows the focused images. Figure 9. shows the 3D reconstructed image and also XY projections of the point targets.

¹ We are grateful to Prof. Iain Mason and Naomi Osman, for supplying this acoustic data from their test facility at Sydney University.

² The simulator utilised was written for flying radar platform applications, and the speed is chosen to obtain a defined sample spacing, together with the radar pulse repetition frequency (prf).

Three-dimensional borehole radar imaging using synthetic aperture time-domain focusing

In the simulation setup there is no ambiguity problem present. The simulation result shows the exact 3D reconstruction of the scene. From the real acoustic focused data we can see the presence of off-nadir axis point scatterers. In the real experiment we have overlay problem, which degrades the 3D reconstructed image.

Conclusions and future work

We need a high signal to noise ratio to apply the algorithm, otherwise image quality is degraded. We are considering straight-line propagation of the wave to calculate the azimuth and slant range position: in real situation we need an accurate EM propagation model. Further work is required to develop an algorithm for resolving layover ambiguities using multiple boreholes.

References

- Bamler, R., Hartl, P., 1998. Synthetic aperture radar interferometry, *Inverse Problems*, 14:R1-R54
- Lopez-Sanchez, J. M., Fortuny-Guasch, J., 2000. 3-D Radar Imaging Using Range Migration Techniques, *IEEE Trans. on Antennas and Propagation*, Vol. 48, No. 5.
- Mason, I., Osman, N., Liu, Q., Simmat, C., Li, M., 2001. Broadband synthetic aperture borehole radar interferometry, *Journal of App. Geophysics*, Vol 47.
- Inggs, M. R., Mukhopadhyay, P. K., Wilkinson, A. J., 2001. Borehole Interferometric SAR : A preliminary study, *Proc. of the 2001 Inter. Geoscience and Remote Sensing Symposium (IGARSS 2001)*.
- Mukhopadhyay, P. K., Inggs, M. R., Wilkinson, A. J., 2001. Borehole Radar Interferometry, *South African Geophysical Association Conference*.
- Pretorius, C.C., Trewick, W.F., Irons, C., 1997. Application of 3-D seismics to mine planning at Vaal Reefs Gold Mine, number 10 shaft, RSA, *Proc. of Exploration 97 : Fourth Decennial International Conference on Mineral Exploration*. Geological Survey of Canada, Ottawa.
- Ulander, L.M.H., Frolind, P., 1998. Ultra-Wideband SAR Interferometry, *IEEE Trans. on Geoscience and Remote Sensing*. Vol. 36, No. 5.
- Wilkinson, A. J., 1997. Techniques for 3-D surface reconstruction using synthetic aperture radar interferometry, PhD thesis, University of London.

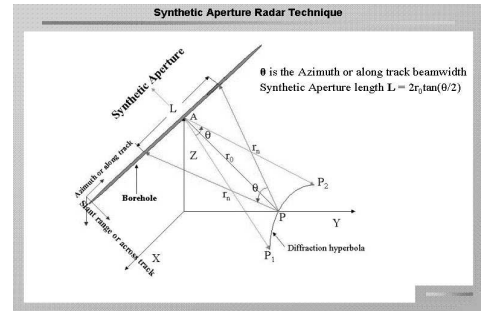


Figure 1.

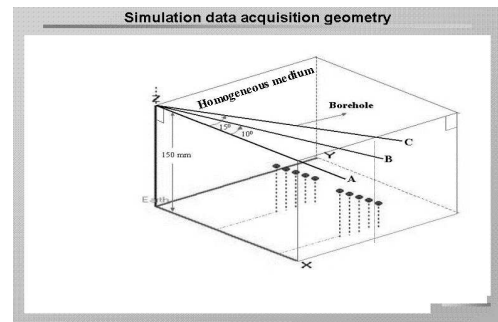


Figure 2.

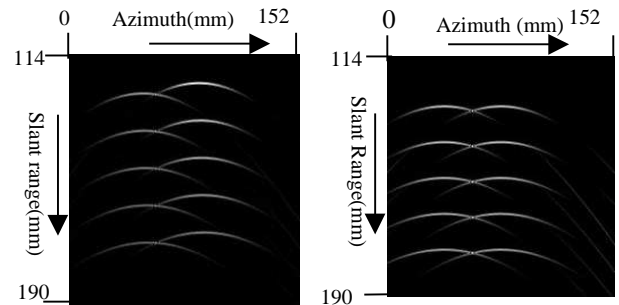


Figure 3(a).
Borehole A

Figure 3(b).
Borehole B

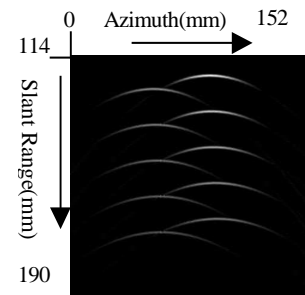


Figure 3(c).
Borehole C

Three-dimensional borehole radar imaging using synthetic aperture time-domain focusing

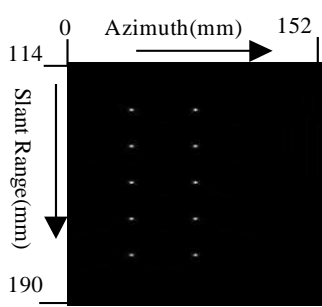


Figure 4(a).

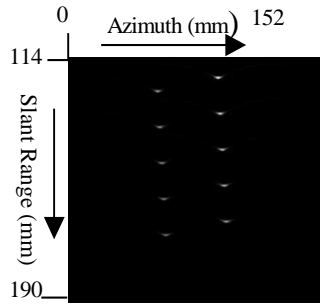


Figure 4(b).

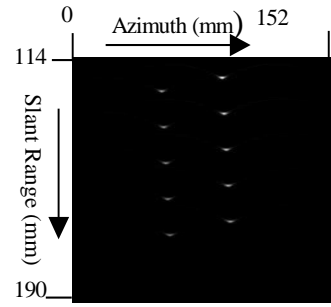
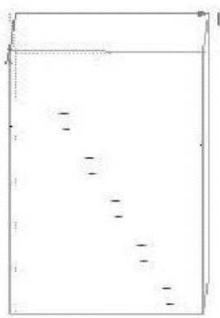
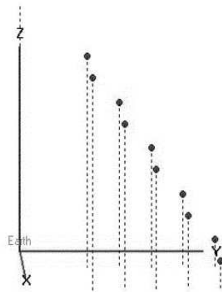


Figure 4(c).



Reconstructed 3D point targets



Input 3D point targets

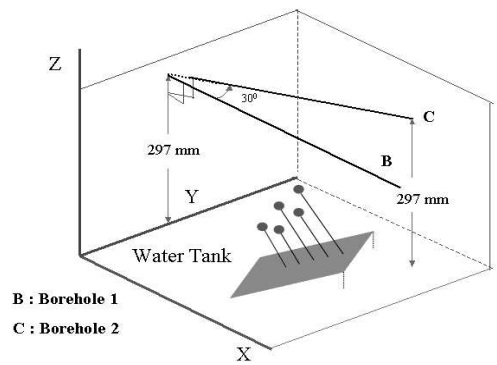


Figure 5.

Figure 6.

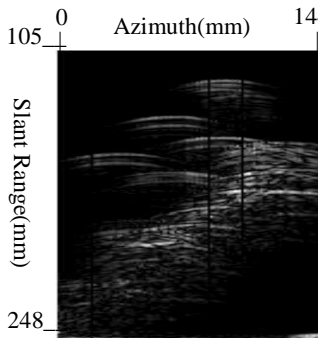


Figure 7(a).

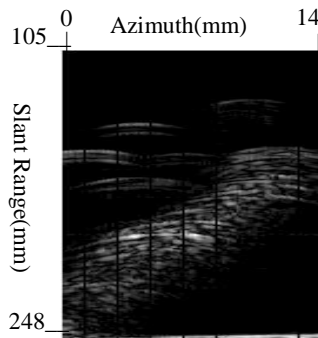


Figure 7(b).

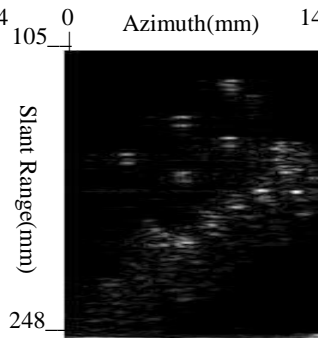


Figure 8(a).

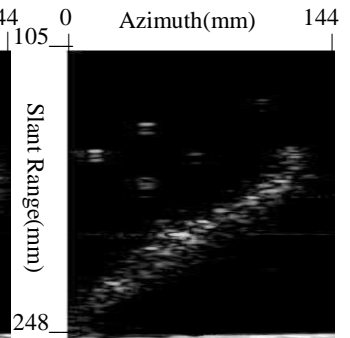


Figure 8(b).

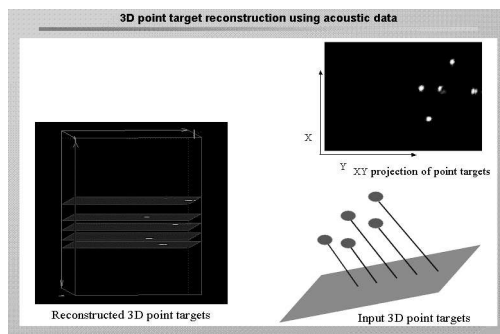


Figure 9.